BIOCHEMISTRY
including biophysical chemistry & molecular biology

Article

pubs.acs.org/biochemistry

Probing the Spatial Organization of Bacteriochlorophyll *c* by Solid-State Nuclear Magnetic Resonance

Shih-Chi Luo,[†] Yadana Khin,[§] Shing-Jong Huang,[‡] Yanshen Yang,[§] Tsai-yi Hou,[†] Yuan-Chung Cheng,[†] Hao Ming Chen,[†] Yi-Ying Chin,[∥] Chien-Te Chen,[∥] Hong-Ji Lin,[∥] Joseph Kuo-Hsiang Tang,*[,§] and Jerry Chun Chung Chan*[,†]

[†]Department of Chemistry and [‡]Instrumentation Center, National Taiwan University, Taipei 10617, Taiwan

[§]Department of Chemistry and Biochemistry, Clark University, Worcester, Massachusetts 01610, United States,

[∥]National Synchrotron Radiation Research Center, Hsinchu 30076, Taiwan

Supporting Information

ABSTRACT: Green sulfur bacteria, which live in extremely low-light environments, use chlorosomes to harvest light. A chlorosome is the most efficient, and arguably the simplest, light-harvesting antenna complex, which contains hundreds of thousands of densely packed bacteriochlorophylls (BChls). To harvest light efficiently, BChls in a chlorosome form supramolecular aggregates; thus, it is of great interest to determine the organization of the BChls in a chlorosome. In this study, we conducted a ^{13}C solid-state nuclear magnetic resonance and Mg K-edge X-ray absorption analysis of chlorosomes from wild-type *Chlorobaculum tepidum*. The X-ray absorption results indicated that the coordination number of the Mg in the chlorosome must be >4, providing evidence that electrostatic interactions formed between the Mg of a BChl and the carbonyl group or the hydroxyl group of the neighboring BChl molecule. According to the intermolecular distance constraints obtained on the basis of ^{13}C homonuclear dipolar correlation spectroscopy, we determined that the molecular assembly of BChls is dimer-based and that the hydrogen bonds among the BChls are less extensive than commonly presumed because of the twist in the orientation of the BChl dimers. This paper also reports the first ^{13}C homonuclear correlation spectrum acquired for carotenoids and lipids—which are minor, but crucial, components of chlorosomes—extracted from wild-type *Cba. tepidum*.

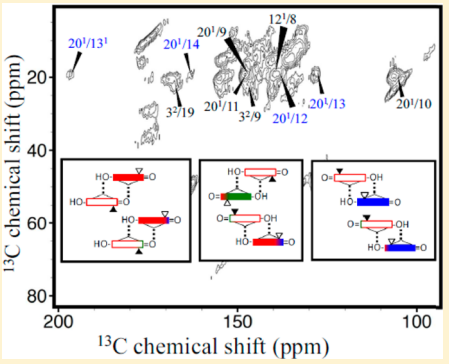

Green sulfur bacteria, which live in extremely low-light environments,[1,2] use chlorosomes to harvest light and perform photosynthesis.[3,4] A chlorosome, which is attached to the inner phase of the cytoplasmic membrane,[5] is the most efficient, and arguably the simplest, light-harvesting antenna complex.[6] Unlike other light-harvesting species, which are protein−pigment complexes, the chlorosome is a pigment−pigment complex that contains up to 250,000 copies of self-assembled bacteriochlorophylls (BChls)[7] that were suggested to be arranged as J-type aggregates.[8] The strong excitonic coupling in the aggregates leads to a red-shift of up to 90 nm for the Q_y absorption band of the BChls in the chlorosome (from 667 to 750 nm).[9,10] To harvest light efficiently, BChls in the chlorosome exist as supramolecular aggregates.[11] Moreover, chlorosomes are resistant to heat, variation in pH, high ionic strengths, and photodegradation;[7,12−14] thus, they are excellent targets for developing biomimetic photosynthetic systems.

Although a chlorosome is the most efficient light-harvesting complex, its molecular structure is not fully understood. Because of difficulties in obtaining sizable single crystals of chlorosomes, solid-state NMR is the most powerful physical technique available for investigating structural information relevant to the BChls in a chlorosome.[15−23] Several structural models have been proposed for the chlorosomes in the green sulfur bacteria *Chlorobaculum tepidum* and *Chlorobium limicola*. According to the model proposed by Nozawa et al., the *Cba. tepidum* chlorosome is assembled in parallel layers comprising piggyback BChl *c* dimers.[15] The chlorosome models proposed for *Chl. limicola* were also dimer-based.[20,22] By contrast, Ganapathy et al. argued that the chlorosome from the *bchQRU* mutant of *Cba. tepidum* was formed by syn- and antimonomeric building blocks of BChls,[21] which is termed the syn−anti model in this study. The descriptors "syn" and "anti" are defined by whether the orientation of the Mg^{2+} ion ligated to the C-3^1 hydroxyl group of an adjacent BChl molecule is on the same (syn) or opposite (anti) side of the esterifying alcohol. Although the *bchQRU* mutant can synthesize a uniform BChl homologue and greatly enhance the NMR spectral resolution of the chlorosome,[21] the light-harvesting efficiency of the mutant is inferior to that of the wild-type (WT) species in low-light environments.[24] Thus, it is unclear whether the structure established for a mutant is relevant to that of the WT species.

Received: June 17, 2014
Revised: August 1, 2014
Published: August 10, 2014

dx.doi.org/10.1021/bi500755r | *Biochemistry* 2014, 53, 5515−5525

Indeed, characterizing the origin of the inherent structural disorder of the WT chlorosome of *Cba. tepidum* might help unravel how excitation energy is efficiently transferred in extremely low-light environments.

In this study, we used ^{13}C solid-state NMR and Mg K-edge X-ray absorption spectroscopies to probe the spatial organization of BChls in the chlorosome of WT *Cba. tepidum*. Our structural models were verified by simulating the optical absorption spectra of the corresponding clusters consisting of 12 BChl *c* molecules. We demonstrated that (i) the syn−anti model derived for the *bchQRU* mutant cannot appropriately describe the assembly of BChls in the WT chlorosome, (ii) the molecular assembly of the BChls in the WT chlorosome is dimer-based and the two BChls do not conform to the parallel or antiparallel alignment as described in other studies,[20−23] and (iii) the hydrogen bonds among the BChls are less extensive than commonly presumed because of the twist in the orientation of the BChl dimers. We also identified the first ^{13}C homonuclear correlation spectrum acquired for carotenoids and lipids—which are minor, but crucial, components of chlorosomes—extracted from WT *Cba. tepidum*.

MATERIALS AND METHODS

Sample Preparation. $NaH^{13}CO_3$ and $^{15}NH_4Cl$ were obtained from Cambridge Isotope Laboratories (Andover, MA). All other chemicals were obtained from Sigma-Aldrich and used as received without further purification. *Cba. tepidum* was cultured as described in the literature,[4] supplied with $NaH^{13}CO_3$ and $^{15}NH_4Cl$. In brief, the cultures were incubated at 45 °C in low-intensity light (100 ± 10 μmol m^{-2} s^{-1}) and harvested at the steady state of growth, from which chlorosomes were extracted from the membrane fraction using NaI (2 M) followed by sucrose gradient separation via ultracentrifugation at 135000*g* for 16 h. The ^{13}C- and ^{15}N-labeled chlorosome was sedimented in 35−45% of sucrose layers, whereas the unlabeled chlorosome was found in 25−35% of sucrose layers. The purified chlorosomes were desalted and lyophilized, and approximately 20 mg of the lyophilized chlorosome sample was obtained per liter of culture. The chlorosome samples were characterized by room-temperature UV−visible, fluorescence emission, and circular dichroism (CD) spectroscopy and dynamic light scattering (DLS) as reported previously.[7,14] ^{13}C-labeled carotenoids were extracted by methanol from the ^{13}C-enriched culture, in which $NaHCO_3$ was replaced with $NaH^{13}CO_3$. The BChls in the methanol extract were removed using an aluminum oxide column.[25] Carotenoids were collected by monitoring the absorbance at 490 and 460 nm. Approximately 2 mg of labeled carotenoids was obtained from 1 L of culture.

NMR Measurements. All NMR experiments were conducted at ^{13}C and ^{1}H frequencies of 600 MHz on a Bruker AVIII600 NMR spectrometer equipped with commercial 3.2 mm probes. The measurements were taken at 275 K. The sample was confined in the middle of the rotor volume using Teflon spacers. The $^{13}C-^{13}C$ dipolar correlation experiments were conducted using the 3.2 mm probe at a spinning frequency of 12.5 kHz. The sample mass was 11 mg. For the $^{13}C\{^{1}H\}$ cross-polarization, the ^{1}H nutation frequency was linearly ramped from 40 to 50 kHz and that of ^{13}C optimized for the Hartmann−Hahn matching condition.[26] The contact time was set to 1.5 ms. The radiofrequency-driven recoupling (RFDR) technique was employed to achieve homonuclear polarization transfer.[27] The π pulse (6.7 μs) trains were phase cycled according to the XY-16 scheme.[28] The mixing time was set to 1.28 or 3.84 ms. Quadrature detection in the F_1 dimension was achieved by the States−TPPI approach. For each t_1 increment, 64 transients were collected and a total of 128 increments were collected at steps of 26.67 μs. The recycle delay was set to 2 s. Two-pulse phase-modulated (TPPM) decoupling[29] of 85 kHz was set during the t_1 and t_2 evolution periods, and the continuous-wave proton decoupling of the same strength was applied during the mixing time. ^{13}C NMR chemical shifts were referenced to tetramethylsilane (TMS), using adamantane as the secondary reference standard.

Mg K-Edge X-ray Absorption. The Mg K-near-edge X-ray absorption fine structure (NEXAFS), also commonly termed X-ray absorption near-edge structure (XANES), experiments were performed at the Dragon Beamline of the National Synchrotron Radiation Research Center (NSRRC) in Taiwan. The photon source was provided by a bending magnet and monochromatized by a spherical grating monochromator with 1200 lines/mm. The desalted and lyophilized chlorosomes were used in the measurements. The entrance slit was optimized to produce the best signal-to-noise ratio, in which a slit of 0.05 mm was employed with a 1.18 eV photon energy resolution at the Mg K-edge ($h\nu \approx 1300-1340$ eV). The spectrum was recorded at room temperature via the total electron yield (TEY) method by recording the total draining current, in which the sample powders were mounted over the carbon tape. For the data analysis, a smooth pre-edge function was subtracted to eliminate the instrumental background and the absorption from other edges. The spectra were normalized by the corresponding edge jump (Mg K-edge) to eliminate the concentration effect.

Modeling of the Absorption Spectrum. To calculate the absorption spectrum based on the structural data, we considered a system of *N* BChls described by the following Frenkel exciton Hamiltonian:

$$H = \sum_{n=1}^{N} E_n |n\rangle\langle n| + \sum_{n\neq m} J_{nm} |n\rangle\langle m|$$

where $|n\rangle$ denotes a BChl Q_y excited state localized at the *n*th BChl, E_n is the excitation energy of $|n\rangle$, and J_{nm} is the excitonic coupling between $|n\rangle$ and $|m\rangle$. We adopted the dipole−dipole approximation to calculate the excitonic coupling J_{nm} based on the structural data:

$$J_{nm} = f\left[\frac{\vec{\mu}_n \cdot \vec{\mu}_m}{|\vec{R}_{nm}|^3} - 3\frac{(\vec{\mu}_n \cdot \vec{R}_{nm})(\vec{\mu}_m \cdot \vec{R}_{nm})}{|\vec{R}_{nm}|^5}\right]$$

where $\vec{R}_{nm} = \vec{R}_n - \vec{R}_m$ is the Mg−Mg distance of the two BChls, $\vec{\mu}_n$ is the transition dipole moment of the BChl Q_y excitation $|n\rangle$, and $f = 0.8$ is a scaling factor that describes the screening of the Coulomb coupling by the dielectric environment.[30] In this work, we used a BChl *c* dipole strength of 16.4 D^2.[31] Furthermore, we assumed equal site energies for all the BChls in the cluster ($E_n = 0$) and assumed that the transition dipoles of the Q_y excitations were aligned along the direction shown in Figure 1. We then calculated the full exciton Hamiltonian *H* as an $N \times N$ matrix, followed by diagonalizing *H* numerically to obtain eigenstates that are responsible for light absorption:

dx.doi.org/10.1021/bi500755r | *Biochemistry* 2014, 53, 5515−5525

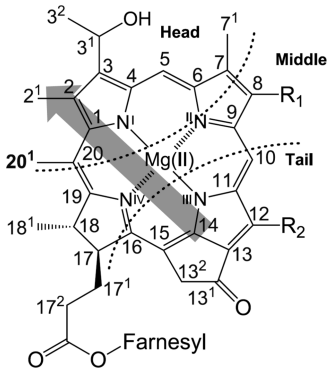

Figure 1. Structure of BChl *c* homologues (R_1 = ethyl, propyl, isobutyl, or neopentyl; R_2 = methyl or ethyl), with the monomeric Q_y transition dipole moment shown as an arrow. The carbons are categorized into three groups, viz., head, middle, and tail.

$$H|\phi_\alpha\rangle = \varepsilon_\alpha|\phi_\alpha\rangle$$

where ε_α is the excitation energy of the αth exciton state and the delocalized eigenfunction $|\phi_\alpha\rangle$ written as a superposition of the site-localized states:

$$|\phi_\alpha\rangle = \sum_n c_n^\alpha |n\rangle$$

Thus, the transition dipole moment of $|\phi_\alpha\rangle$ was obtained as

$$\overrightarrow{M_\alpha} = \sum_n c_n^\alpha \overrightarrow{\mu_n}$$

and the absorption spectrum of the excitonic system was subsequently approximated as a sum of sticks:

$$I_\alpha(\omega) = \sum_\alpha |\overrightarrow{M_\alpha}|^2 \delta(\omega - \varepsilon_\alpha)$$

RESULTS

Sample Characterization. Figure 1 illustrates the structure of BChl *c* homologues and the orientation of the monomeric Q_y transition dipole moment. The purified chlorosomes and carotenoids of *Cba. tepidum* were characterized by a series of physical methods. The absorption spectra of the chlorosome and carotenoids are shown in Figure 2. For the UV−visible spectrum of carotenoids, the absence of any spectral component near 667 nm (the Q_y band of BChl *c* monomers) indicated that BChls had been largely removed in the preparation of carotenoids. The fluorescence emission spectrum and the dynamic light scattering data of our chlorosome sample were consistent with the literature results reported for *Cba. tepidum* (Figure S1 of the Supporting Information).

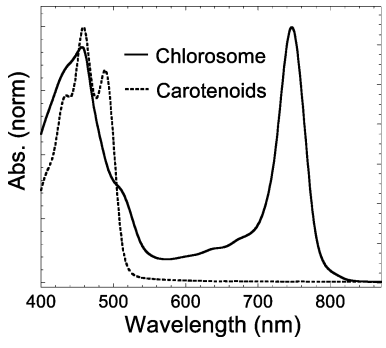

Figure 2. Absorption spectra of the chlorosome and carotenoids.

^{13}C Chemical Shifts of the Chlorosome. The $^{13}C-^{13}C$ correlation spectrum was acquired for our chlorosome sample, and the overall spectral assignment is given in Figures S2−S5 of the Supporting Information. Although the structural heterogeneity of the chlorosomes of WT *Cba. tepidum* was found to be quite substantial by cryo-EM microscopy,[21] the line width of the ^{13}C NMR signals, in the range of 1.5−3 ppm, revealed that the level of local structural order of the BChl molecules remains reasonably high. The ^{13}C chemical shifts of BChl *c* obtained in this work and those reported for BChl *c* in the literature are summarized in Table 1,[17,20,23] in which a splitting of the ^{13}C NMR signals was found for certain regions of the macrocycle. These doublets are a direct consequence of the structural arrangement of BChl *c* in the chlorosome.[19,32] Via comparison of the regions in which signal doubling occurred, we suggested that the structural arrangement of the BChl *c* molecules of *Cba. tepidum* and *Chl. limicola* is similar. Interestingly, the pattern of signal doubling observed for WT *Cba. tepidum* is considerably different between our data and those reported by Ganapathy and co-workers,[23] although our ^{13}C chemical shift data are largely consistent with their results.

A more careful examination of Table 1 revealed that the chemical shift of C-8^1 was remarkably different between *Cba. tepidum* and *Chl. limicola*. Both *Cba. tepidum* (a thermophilic green sulfur bacterium) and *Chl. limicola* (a mesophilic green sulfur bacterium) produce BChl *c* homologues with four different C-8^1 substituents, viz., ethyl, propyl, isobutyl, and neopentyl. It was reported that the *bchQR* mutant of *Cba. tepidum*, which produces only an ethyl substituent at C-8 of BChl *c*, exhibits a chemical shift of 19.2 ppm at C-8^1.[23] That is, the chemical shift of C-8^1 is very similar for the WT and mutants of *Cba. tepidum*. This observation is consistent with the suggestion that the ethyl substituent at C-8 is the dominant homologue in *Cba. tepidum*.[33] In comparison, the C-8^1 chemical shift of BChl *c* in *Chl. limicola* is deshielded by almost 10 ppm relative to that in *Cba. tepidum* (see Table 1). Therefore, it could be inferred that *Chl. limicola* produced a substituent at C-8 that was bulkier that of *Cba. tepidum*. On the other hand, the chemical shift of C-12^1 was found to be around 18 ppm for WT *Cba. tepidum* and *Chl. limicola*, but 10.4 ppm for *bchQR Cba. tepidum*. Because WT *Cba. tepidum* produces either an ethyl or methyl substituent at C-12 of BChl *c*, whereas the mutants produce only a methyl substituent,[24] we concluded that the substituent at C-12 must be an ethyl group for WT *Cba. tepidum* and *Chl. limicola*. Consistently, we observed that the chemical shifts of C-8^1 and C-12^1 are very similar for WT *Cba. tepidum*.

Chemical Shifts of Carotenoids and Lipids. In addition to BChls, chlorosomes contain other minor but important components such as carotenoids.[3,34] It was suggested that carotenoids could protect chlorosomes from photodegradation,[12] and the abundance of carotenoids in the chlorosome was estimated to be ∼10% of the amount of BChls.[35] The major species of carotenoids in *Cba. tepidum* is chlorobactene,[36] which could be well within van der Waals contact range of BChl *c*.[37,38] Judging from the chemical structures of BChl and chlorobactene, one may expect that there is a considerable spectral overlap between their NMR signals. To identify the signals arising from carotenoids, we painstakingly extracted the carotenoids from the ^{13}C-labeled chlorosomes with methanol.

dx.doi.org/10.1021/bi500755r | *Biochemistry* 2014, 53, 5515−5525

Table 1. Summary of the ^{13}C Chemical Shifts (parts per million) of BChl *c*[a]

carbon	classification	WT *Cba. tepidum* (this work)	WT *Cba. tepidum*[23]	*bchQR Cba. tepidum*[23]	WT *Chl. limicola*[20]
C-1	H	154.1	153.8	151.6	153.7
C-2	H	135.2	134.7	132.9	134.8
C-2^1	H	14.7	14.4	11.3	14.5
C-3	H	140.3	140.1	137.4	139.7
C-3^1	H	(64.4, 63.7)	63.7	(62.1, 61.4)	(64.1, 63.3)
C-3^2	H	(25.6, 23.5)	23.4	(17.6, 16.7)	(24.9, 22.5)
C-4	H	(145.0, 144.0)	(144.6, 143.9)	(141.9, 141.5)	(143.9, 144.6)
C-5	H	(102.1, 96.5)	(102, 97)	(100.9, 93.5)	(101.6, 95.6)
C-6	H	(150.9, 149.8)	(149.9, 149.5)	(147.5, 146.8)	(150.5, 150.2)
C-7	H	(133.5, 132.1)	(133.2, 131.9)	(131.5, 130.0)	(132.5, 132.0)
C-7^1	H	(10.8, 7.8)	(11, 7.7)	(10.4, 7.5)	(11, 7.1)
C-8	M	(141.2, 139.9)	(139.2, 138.2)	140.3	(141.4, 139.7)
C-8^1	M	(19.2, 17.5)	18	19.2	(29.9, 28.0)
C-9	M	147.3	147.5	144.4	146.7
C-10	T	105.5	105.9	103.6	105.8
C-11	T	147.9	146.8	146.0	147.4
C-12	T	139.1	139	130.1	138.6
C-12^1	T	17.9	18.6	10.4	18.7
C-13	T	128.1	127.4	126.8	127.8
C-13^1	T	196.5	196.5	(194.8, 191.3)	196
C-13^2	T	48.5	49.3	47.9	48.4
C-14	T	162.7	162.7	(162.1, 159.2)	162.4
C-15	T	104.6	103.8	102.8	104
C-16	T	156.0	(154.3, 154.1)	152.5	154.7
C-17	M	49.4	(49.0, 48.9)	(51.3, 48.9)	50.2
C-17^1	M	29.3	–	30.4	30.9
C-17^2	M	29.3	–	30.4	29.6
C-17^3	M	173.5	–	–	174.5
C-18	M	(48.1, 46.8)	48.3	47.6	(48.8, 46.0)
C-18^1	M	(21.0, 20.4)	21.1	20.7	(21.1, 20.4)
C-19	M	(167.8, 166.5)	(169.7, 167.5)	(167.2, 164.3)	(167.3, 165.9)
C-20	H	(106.7, 105.4)	(105, 103.7)	(103.2, 101.4)	(104.4, 103.7)
C-20^1	H	19.1	20.3	(20.7, 20.3)	(21.9, 21.5)

[a]The data in parentheses represent the signal doubling observed for the carbons. The regions of head (H), middle (M), and tail (T) are indicated in Figure 1.

Figure 3 illustrates the $^{13}C-^{13}C$ correlation spectrum acquired for the methanol extract at 273 K. Although a detailed assignment of the spectrum is very difficult, we had identified the characteristic signal regions of the carotenoids on the basis of the correlation patterns at ~30 and ~130 ppm.[16,39] However, the signals in the region of 173 ppm were not assigned to carotenoids, which do not contain any carbonyl functional groups. Among those non-BChl components in the chlorosome of green sulfur bacteria, the most abundant species are lipids (11%) and proteins (27%).[3] Because the fraction of proteins should have been removed during the process of methanol extraction, the carbonyl carbon signals were assigned to lipids. In Figure 3, we identify certain spectral features that can be assigned to carotenoids and lipids. Although the signal-to-noise ratio of our chlorosome spectrum precluded their manifestation, the spectral information could be useful for further investigation of the spatial proximity among BChls, lipids, and carotenoids in the chlorosome.

Intermolecular Distance Constraints. On the basis of the chemical shift assignments summarized in Table 1, we had identified the intermolecular contacts for BChl *c* of WT *Cba. tepidum*. Figure 4 illustrates the excerpt of the $^{13}C-^{13}C$ correlation spectrum of our sample acquired using the technique of RFDR. For the sake of simplicity, we labeled only the peaks assigned to intermolecular contacts. The intermolecular contacts that had been reported in the literature are labeled in black.[20,22,23] Most of the new contacts observed in this study, labeled in blue, were assigned to the interacting pairs involving C-20^1. A careful examination of the raw spectra reported for WT *Chl. limicola* revealed that the intermolecular contacts involving C-20^1 were also detected in that species.[22] Table 2 summarizes the intermolecular distance constraints obtained for *Cba. tepidum* and *Chl. limicola*. Note that relatively few intermolecular contacts had been reported for the mutants of *Cba. tepidum*, although the spectral resolution of the *bchQRU* and *bchQR* chlorosomes is significantly better than that of the WT chlorosome.[21,23] In particular, the C-7^1/C-18 and C-7^1/C-18^1 intermolecular contacts were observed in the $^{13}C-^{13}C$ correlation spectrum of the *bchQRU* chlorosome,[21] but not in the spectrum of the WT chlorosome.

First Coordination Shell of Mg. Figure 5 shows the Mg K-edge XANES spectra of the chlorosome, spinel,[40] and lizardite.[41] Because it is very difficult to properly interpret an Mg K-edge XANES spectrum because of the absence of appropriate references to compare with that of the chlorosome, two model minerals, viz., spinel and lizardite, were used as the reference compounds. Generally, there are three prominent features at the near-edge region from 1300 to 1340 eV, labeled

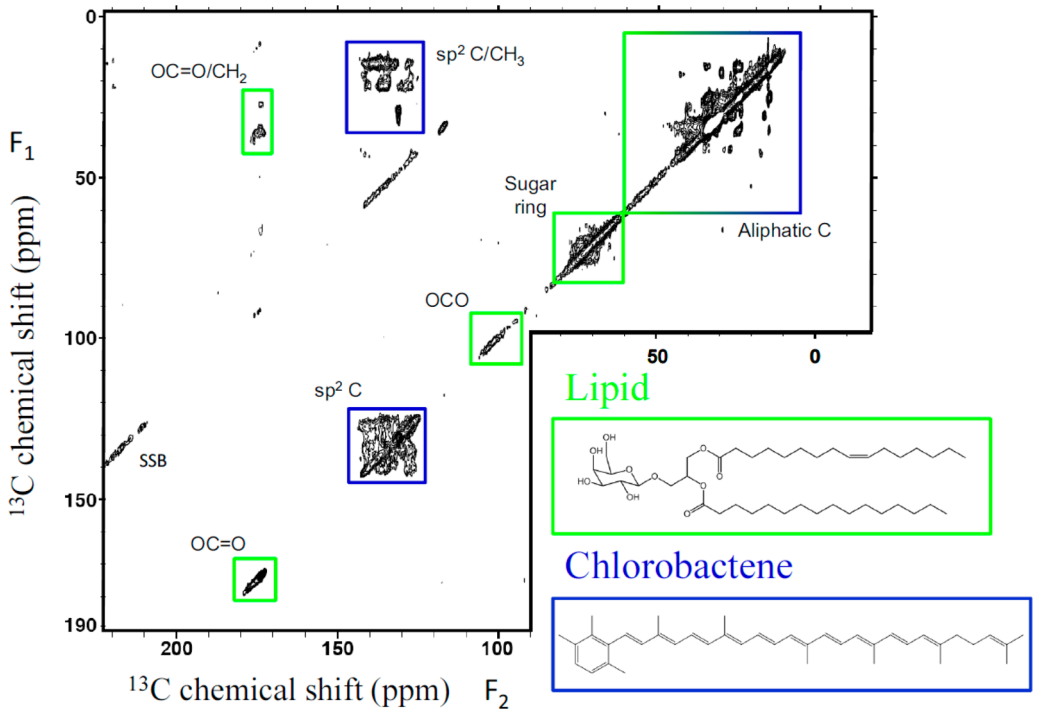

Figure 3. ^{13}C homonuclear dipolar correlation spectrum of the carotenoids and lipids of WT *Cba. tepidum*. The spinning side bands are denoted by SSB.

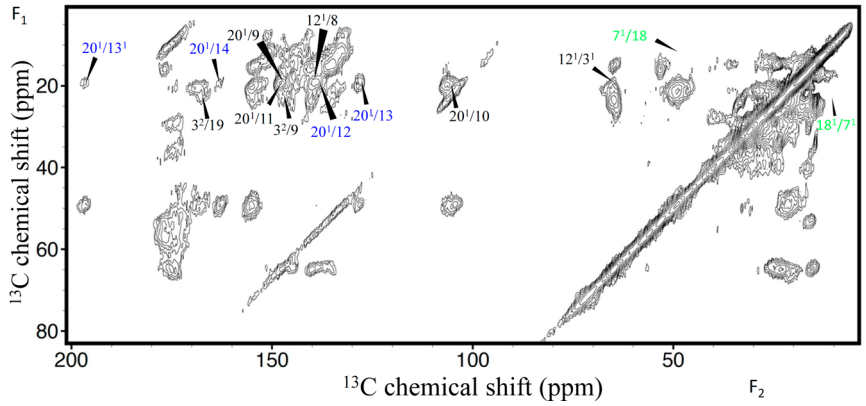

Figure 4. Excerpt of the ^{13}C homonuclear dipolar correlation spectrum of the chlorosome sample. The intermolecular constraints between C-20^1 and C-12, C-13, C-13^1, and C-14, which have not yet been reported in the literature, are labeled in blue; those that have been reported in the literature are labeled in black. The expected regions of C-7^1/C-18 and C-18^1/C-7^1, which are the key contacts for the syn−anti model, are highlighted in green.

as A−C. Peak A is assigned to the electronic transition from 1s to an empty 3p orbital of the Mg atom, whereas peak B corresponds to the transitions from the 1s orbital to the hybridized orbitals within ligand and absorbing atoms. In addition, peaks A and C are related to the multiple scatterings from the coordination shells around the absorbing Mg atoms. By comparing the minerals of spinel and lizardite, in which the central absorbing Mg atoms are coordinated by four and six oxygen atoms, respectively, Trcera et al. demonstrated that the coordination of the absorbing atoms would affect the position of the first main absorption (peak A).[42] For our chlorosome sample, peak A was shifted to an energy higher than that of spinel but rather similar to that of lizardite. This observation suggested that the coordination numbers of Mg atoms in the chlorosome are >4. However, it should be cautioned that the experimental conditions of our XANES spectrum collected for chlorosomes are not entirely identical to those for spectra reported for spinel and lizardite, so further investigation may be required to validate the interpretation of our data. Meanwhile, a pentacoordinated Mg ion with a hydroxide ion bound was suggested by computational studies by Kluge and Weston,[43] and Mg ions with coordination numbers of >4 have been found in chlorophylls in light-harvesting complex II.[44] Interpretation of the spectral positions of peaks B and C in Figure 5 would require more detailed theoretical simulations that are beyond the scope of this work.

Cabaret et al. conducted quantitative multiple scattering calculations at the Mg K-edge of diopside.[45] The XANES spectrum of diopside is also characterized by peaks A−C. As the cluster radius of the simulation model decreased from 8 to 3 Å, the spectral feature of the calculated XANES spectrum became less prominent. This result suggested that an absence of

dx.doi.org/10.1021/bi500755r | *Biochemistry* 2014, 53, 5515−5525

Table 2. Intermolecular $^{13}C-^{13}C$ Correlation Signals Reported for BChls *c* in Different Mutants of *Cba. tepidum* and Other Bacterial Species[a]

intermolecular contact	constraint type[b]	WT *Cba. tepidum* (this work)	*bchQRU Cba. tepidum*[21]	*bchQR Cba. tepidum*[23]	WT *Chl. limicola*[20,22,b]
C-3^2/C-9	H/M	+			+
C-3^2/C-19	H/M	+			
C-12^1/C-3^1	T/H	+	+	+	
C-12^1/C-8	T/M	+			
C-20^1/C-9	H/M	+			+
C-20^1/C-10	H/T	+			
C-20^1/C-11	H/T	+			+
C-20^1/C-12	H/T	+			*
C-20^1/C-13	H/T	+			*
C-20^1/C-13^1	H/T	+			*
C-20^1/C-14	H/T	+			
C-2^1/C-12^1	H/T		+		
C-7^1/C-17	H/M		+		
C-7^1/C-18	H/M		+		+
C-7^1/C-18^1	H/M		+		
C-8^2/C-18	M/M		+		
C-12^1/C-3^2	T/H		+	+	

[a]A plus sign indicates the observation of the corresponding correlation peak. [b]Additional constraints can be found in the cited reference. Asterisks denote the peaks that could be identified in the published spectra but were not assigned by the authors.

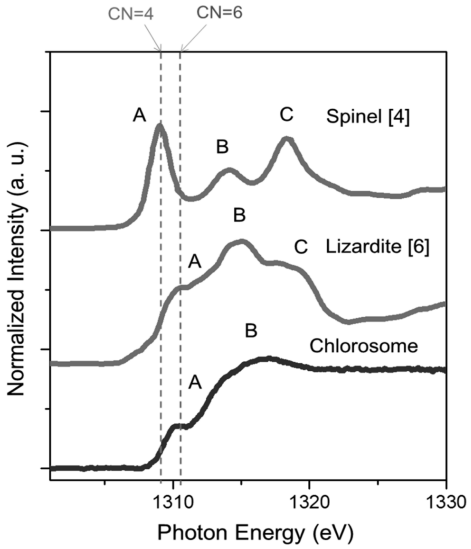

Figure 5. Experimental isotropic Mg K-edge XANES spectra of $MgAl_2O_4$ (spinel), $Mg_3Si_{1.83}Al_{0.17}O_5(OH)_4$ (lizardite), and a chlorosome. The spectra of spinel and lizardite were taken from refs 40 and 41, respectively. The numbers in brackets indicate the coordination numbers of the Mg ion.

long-range order would lead to a featureless K-edge XANES spectrum, because of the relatively weak scattering amplitude from the coordination shell. Consequently, the XANES spectrum obtained for our sample was consistent with the intrinsic disordered nature of the chlorosome. Overall, the Mg K-edge XANES spectrum demonstrated that Mg atoms in the chlorosome have a coordination number of >4.

DISCUSSION

Intermolecular Contacts Involving C-20^1. The syn−anti model proposed by Ganapathy et al. was constructed on the basis of the two crucial intermolecular contacts of BChl *c* molecules, C-7^1/C-18 and C-7^1/C-18^1, observed for the *bchQRU* chlorosome.[21] In our NMR measurements of the WT *Cba. tepidum* chlorosomes, however, we could not observe these two intermolecular contacts, even though longer mixing times and other dipolar recoupling techniques were used (data not shown). On the other hand, the key intermolecular contacts we obtained for WT *Cba. tepidum* mostly involved C-20^1 and corresponded to the distance constraints between the head and tail regions. These contacts were not observed for the *bchQRU* mutant because the C-20^1 moiety had been replaced by a hydrogen.[21] Considering the fact that the pattern of signal doubling of the WT and *bchQR* chlorosomes is different (Table 1), we concluded that the syn−anti model proposed by Ganapathy et al. is not appropriate for WT *Cba. tepidum*.

The multiple interactions of C-20^1 with adjacent BChl molecules found in our study implied that C-20^1 plays a crucial role for the packing of BChls in the WT *Cba. tepidum* chlorosome. With the knowledge that the only difference between BChl *c* and BChl *d* is that the C-20^1 group of BChl *c* is absent in BChl *d*, it is likely that BChl *d*-type chlorosomes exhibit spatial organizations different from those of BChl *c*-type chlorosomes. Previous studies showed that the absence of C-20^1 leads to a blue-shift of the Q_y absorption band of the chlorosome and BChl *d*-producing green sulfur bacteria grow slower in low-intensity light than the BChl *c*-containing species.[46] Similar to BChl *c*, BChl *e* homologues also contain the C-20^1 moiety. Several BChl *e*-producing green sulfur bacteria were discovered down to 100 m below the surface of the Black Sea.[2] It was shown recently that the species containing BChl *f*, which is BChl *e* without the C-20^1 moiety, also harvest photons less efficiently than species containing BChl *e*.[47,48] Consequently, we believe that the C-20^1 group, which is crucial for the molecular packing in BChl *c* (and perhaps BChl *e*), can enhance exciton transfer in low-light environments.

Structural Models of WT Bacteriochlorophyll *c*. We have constructed four possible structural models that are compatible with our NMR constraints. Each of the models contains 12 BChl *c* molecules generated by PyMOL.[49] The four models are illustrated in Figure 6 using the cartoon symbols modified from those proposed by Koyama and co-workers.[22] A

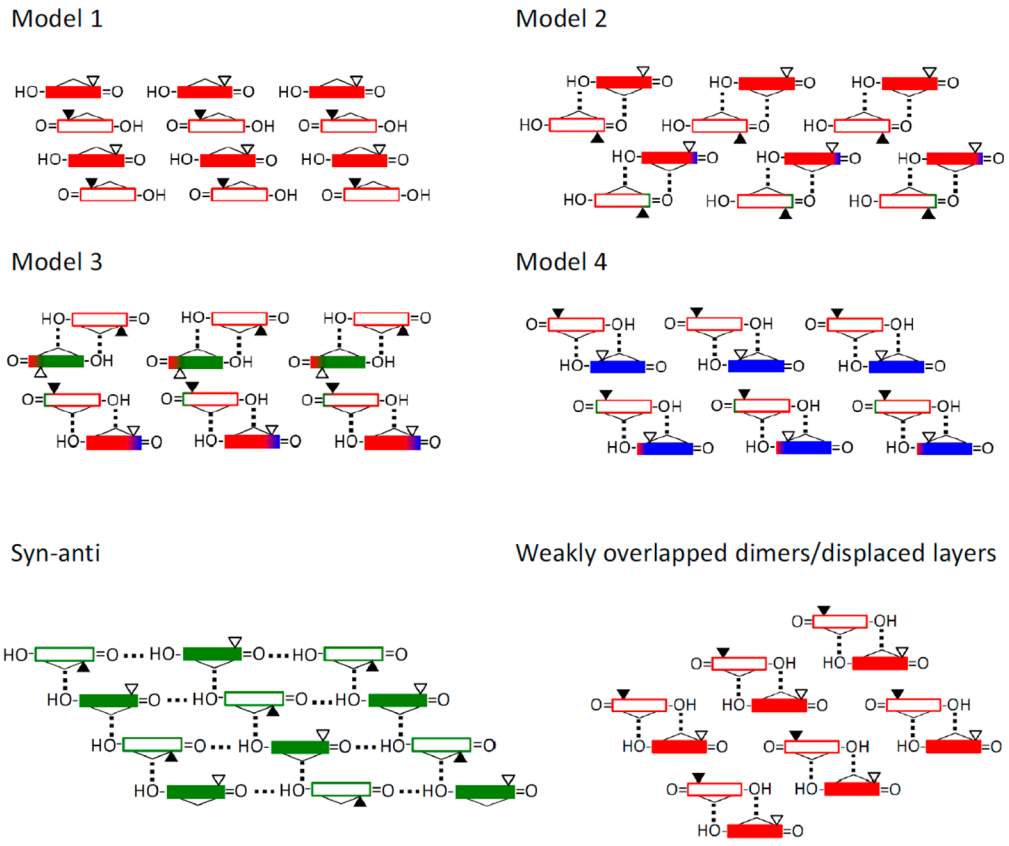

Figure 6. Schematic representation of the four possible structural models of BChl *c* aggregates constructed on the basis of the NMR constraints only (models 1−4): rectangles (the macrocycle), =O (the keto-carbonyl group at C-13^1), −OH (the hydroxyethyl group at C-3), flat triangle (Mg positioned at the apex), and small equilateral triangle (the root of the farnesyl side chain). The cartoons of the macrocycle in six different view angles are represented by three colors combined with filled and empty rectangles. The filled red, green, and blue rectangles represent the macrocycles observed along the direction of $N^{IV} \rightarrow Mg \rightarrow N^{II}$, C-20 → Mg → C10, and C-15 → Mg → C5, respectively. The empty rectangles denote the macrocycles observed from the direction opposite vs that of the filled rectangles. A detailed illustration of the color scheme is given in Figure S6 of the Supporting Information. For comparison, the syn−anti model and the overlapped-dimer model proposed for WT *Cba. tepidum* and *Chl. limicola*, respectively, are reproduced using the same representation scheme.

detailed illustration of our convention is given in Figure S6 of the Supporting Information.

Model 1 is a regular array formed by two alternating stacks of BChl molecules. The orientations of two neighboring BChls belonging to the adjacent stacks differ by a rotation of 180° with respect to the direction normal to the chlorophyll plane. The relative position of the neighboring BChls between two adjacent stacks is determined by the NMR constraints. The bottom two stacks are identical to the top two stacks, except for a horizontal shift in position. The central Mg atom of each BChl molecule is ligated by four nitrogen atoms in model 1. From the Mg K-edge XAS data, however, it is clear that the first coordination shell of Mg contains other coordination partners, in addition to the four nitrogen atoms of the chlorophyll ring. Hence, models 2−4 were constructed with the following additional interactions included:[11,17,50−55] (i) the ligation between the C-3^1 hydroxyl group of one BChl *c* molecule and the central Mg ion of the adjacent BChl molecule (Mg···OH) and (ii) the electrostatic interactions between the C-13^1 carbonyl group of one BChl *c* molecule and the central Mg ion of the adjacent BChl molecule (Mg···O=C). In model 2, the first coordination shell of Mg comprises both Mg···OH and Mg···O=C interactions. The orientations of the BChls within a dimer differ by a rotation of 180° with respect to the axis passing through the N^I, Mg, and N^{III} atoms. Because of the NMR constraints, however, the bottom two stacks must be twisted slightly with respect to the direction normal to the chlorophyll plane, in addition to the horizontal shift in position. The angular twist was manifested as a change in color of the rectangular block in accordance with the representation scheme shown in Figure S6 of the Supporting Information. The dimers of both models 3 and 4 were formed by only the Mg···OH interaction. The most distinguishing feature of these models is that the orientations of the BChls within a dimer differ by a rotation of ∼135° about the normal of the chlorophyll plane. In addition, a significant twist of the dimers about the normal would progress across the stack. The major difference of models 3 and 4 is the orientation of the farnesyl side chains. In model 4, all side chains are pointing upward, whereas in model 3, only half of the side chains are pointing upward. For comparison, we also included the syn−anti and the displaced-layer models proposed for WT *Cba. tepidum* and *Chl. limicola*, respectively, in Figure 6.

Evaluation of the Optical Properties. The validity of the proposed structural models can be evaluated by structure-based simulations of their absorption spectra and a comparison to experimental data. Experimentally, the BChl *c* Q_y absorption maximum in the chlorosome shows a large red-shift relative to the Q_y absorption of monomeric BChl *c*.[16] Therefore, BChls in the chlorosome are often characterized as J-aggregates.[56,57] A

dx.doi.org/10.1021/bi500755r | *Biochemistry* 2014, 53, 5515−5525

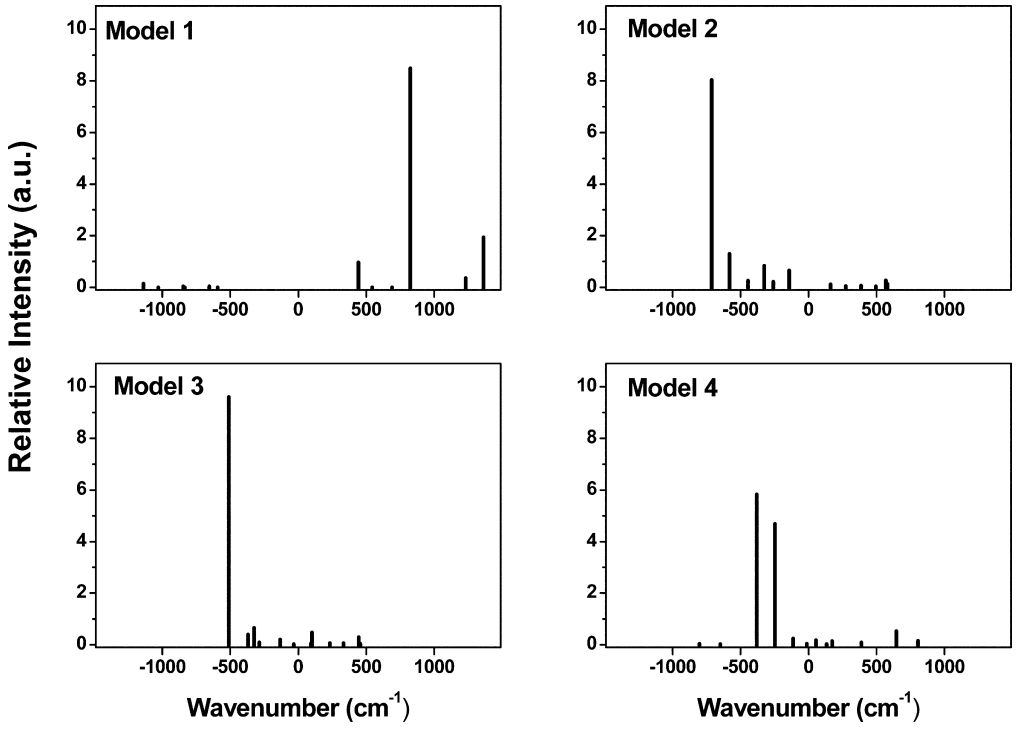

Figure 7. Optical absorption spectra calculated for models 1−4.

reasonable structural model for the chlorosome should exhibit this spectral characteristic. To test our proposed models, we adopted an exciton theory[58] (Materials and Methods) to simulate the optical absorption spectrum of a cluster consisting of 12 BChl *c* molecules based on each of the four structural models depicted in Figure 6. The coordinates of the Mg atoms and the orientations of the corresponding transition dipole moments are listed in Table S1 of the Supporting Information. The excitonic couplings between BChl *c* Q_y transitions were calculated by assuming point−dipole interactions. This approach should yield reasonable results to indicate the signs of the excitonic couplings and the redistribution of transition dipoles in the aggregates.

As shown in Figure 7, our simulated spectra exhibited large red-shifts except for those of model 1. Addition simulations for model 1 with an alternative arrangement of BChls in the middle column also gave a blue-shift (Figure S7 of the Supporting Information). We therefore concluded that the transition-dipole arrangements in model 1 are inconsistent with the optical absorption observed in the chlorosome. On the other hand, the other three models exhibited absorption spectra that are in agreement with the suggested J-aggregates characteristic of BChls in the chlorosome. Note that we aim to perform only a semiquantitative analysis to investigate the general features of the absorption spectra predicted by our structural models. Therefore, details such as exciton−phonon couplings and energy disorder were neglected. In principle, a rigorous theoretical modeling of the aggregate line shape based on the full cylindrical chlorosome structure[59] could provide additional structural information. Nevertheless, the exciton simulations performed here had clearly demonstrated that models 2−4 are consistent with the spectral characteristics of a J-aggregate observed in the chlorosome linear spectra.

Assembly of BChls in Chlorosomes. The first solid-state NMR study of chlorosomes can be traced back to the work by Nozawa et al. in 1991.[15,16] Despite the fact that many studies have been published in the past two decades,[15,16,18−23] some essential issues regarding the molecular assembly of BChls in chlorosomes remain unresolved. Egawa et al. reported the first high-resolution structure of BChl *c* molecules in the *Chl. limicola* chlorosome, for which approximately 90 intermolecular $^{13}C-^{13}C$ distance constraints were obtained by analyzing the polarization-transfer matrix of homonuclear ^{13}C spin-diffusion experiments.[20] The structure of the BChl *c* molecules was categorized as piggyback dimer-based parallel layers.[16] However, the authors indicated in a subsequent study that the model required further refinement because the intermolecular correlation peaks were not unequivocally defined.[22] The revised model, which comprises weakly overlapped dimers forming displaced layers, mainly differs from the previous model in the stacking of the BChl dimers[17,53] (Figure 6). At about the same time, Ganapathy et al. exploited the excellent spectral quality of the *bchQRU* mutant chlorosome and proposed the syn−anti model for the *Cba. tepidum* chlorosome.[21] The most astonishing feature of the syn−anti model is that the stacking of BChls is not dimer-based, which conflicts with results reported for *Chl. limicola*[20,22] and with solution-state NMR studies of BChl *c* isolated from *Cba. tepidum*.[60,61]

As discussed in the foregoing section, the syn−anti model cannot describe the packing of BChls in the WT *Cba. tepidum* chlorosome. Because of the limited spectral resolution of our sample, we could not propose a unique structural model for the WT *Cba. tepidum* chlorosome. Nonetheless, our models exhibited valuable features that can provide crucial insights into understanding the packing of BChls in the WT chlorosome. First, models 2−4 belong to the dimer-based stacking category. Second, the orientations of the BChls of a dimer in models 3 and 4 differ by an angle that is closer to 135° than to 180°. All the structural models proposed for chlorosomes have been based on specific types of parallel or antiparallel alignment of two neighboring BChls. If the C-3 and

dx.doi.org/10.1021/bi500755r | *Biochemistry* 2014, 53, 5515−5525

C-13[1] regions of two adjacent BChl molecules are in the proximity of each other, the formation of hydrogen bonding (OH···O═C) is assumed.[20−23] Although the formation of hydrogen bonds has been partially supported by previous NMR,[17,19] molecular modeling,[11] resonance Raman,[52] and infrared spectroscopy[53] studies, the existence of this hydrogen bonding network has recently been questioned.[55] Because of the orientation twist propagating along the stack, models 3 and 4 indicated that not every lateral pair of neighboring BChls can form hydrogen bonds. Consequently, the packing of the farnesyl side chains, which might involve carotenoids and other minor components in the chlorosome, could also play a role in stabilizing the structure of chlorosomes.[62] Third, if more stacks were included in the model construction, the structure could be extended to either a rodlike[63,64] or an undulating lamellar structure.[65] Experiments characterizing the structural features on a nanometer scale will need to be conducted to refine our models.

CONCLUSION

The molecular structure of the chlorosome of WT *Cba. tepidum* has been characterized by solid-state NMR and Mg K-edge XANES spectroscopies. To the best of our knowledge, Figure 5 represents the first Mg K-edge XANES spectrum reported for the chlorosome, which supports the existence of Mg···OH and Mg···O═C interactions. Although the structural information that can be obtained from the XANES spectrum was limited, it demonstrated that Mg K-edge X-ray absorption spectroscopy is a promising technique for examining the Mg coordination shell, which is vital to understanding the assembly of BChls. On the basis of our spectroscopic data, we constructed three structural models for the chlorosome, which exhibited the expected optical properties of J-aggregates and were consistent with our experimental constraints. The most intriguing feature of our models was the twisting of the dimers along the stacking direction, which is a direct consequence of the intermolecular contacts determined for C-20[1] of a BChl and C-10−C-14 of neighboring BChls. This twisting feature of the BChl orientation might be correlated with the efficient excitation energy transfer in the chlorosomes of WT *Cba. tepidum*.

ASSOCIATED CONTENT

Supporting Information

Seven figures and one table documenting the sample characterization of the wild-type *Cba. tepidum* chlorosomes, assignments of the $^{13}C-^{13}C$ homonuclear dipolar correlation spectra of the chlorosome, the alternative model 1, and calculation of the optical spectral data. This material is available free of charge via the Internet at http://pubs.acs.org.

AUTHOR INFORMATION

Corresponding Authors

*E-mail: jtang@clarku.edu.

*E-mail: chanjcc@ntu.edu.tw.

Author Contributions

S.-C.L., Y.K., and Y.Y. contributed equally to this work.

Funding

This work was financially supported by start-up funds from Clark University (to J.K.-H.T.) and the Ministry of Science and Technology of the Republic of China (100-2628-M-002-009-MY3) (to J.C.C.C.). The NMR measurements were taken at the Instrumentation Center of National Taiwan University (NSC-100-2731-M-002-002-MY2).

Notes

The authors declare no competing financial interests.

ACKNOWLEDGMENTS

We thank Mr. Farrokh Zare and members of the laboratory of J.K.-H.T. for assisting in the preparation of samples. Helpful discussion of the XANES data with Dr. Yael Politi (Max Planck Institute of Colloids and Interfaces) is gratefully acknowledged.

ABBREVIATIONS

BChl *c*, bacteriochlorophyll *c*; CP/MAS, cross-polarization/magic angle spinning; NMR, nuclear magnetic resonance; XANES, X-ray absorption near-edge structure.

REFERENCES

(1) Repeta, D. J., Simpson, D. J., Jorgensen, B. B., and Jannasch, H. W. (1989) Evidence for anoxygenic photosynthesis from the distribution of bacteriochlorophylls in the Black Sea. *Nature 342*, 69−72.

(2) Overmann, J., Cypionka, H., and Pfennig, N. (1992) An extremely low-light adapted phototrophic sulfur bacterium from the Black Sea. *Limnol. Oceanogr. 37*, 150−155.

(3) Blankenship, R. E., and Matsuura, K. (2003) *Antenna complexes from green photosynthetic bacteria* (Green, B. R., and Parson, W. W., Eds.) pp 195−217, Kluwer Academic Publishers, Dordrecht, The Netherlands.

(4) Overmann, J. (2006) *The Family Chlorobiaceae. The Prokaryotes*, 3rd ed., Vol. 7, Springer, New York.

(5) Frigaard, N. U., Voigt, G. D., and Bryant, D. A. (2002) *Chlorobium tepidum* mutant lacking bacteriochlorophyll *c* made by inactivation of the *bchK* gene, encoding bacteriochlorophyll *c* synthase. *J. Bacteriol. 184*, 3368−3376.

(6) Oostergetel, G. T., van Amerongen, H., and Boekema, E. J. (2010) The chlorosome: A prototype for efficient light harvesting in photosynthesis. *Photosynth. Res. 104*, 245−255.

(7) Tang, J. K., Saikin, S. K., Pingali, S. V., Enriquez, M. M., Huh, J., Frank, H. A., Urban, V. S., and Aspuru-Guzik, A. (2013) Temperature and carbon assimilation regulate the chlorosome biogenesis in green sulfur bacteria. *Biophys. J. 105*, 1346−1356.

(8) Sengupta, S., and Wurthner, F. (2013) Chlorophyll J-aggregates: From bioinspired dye stacks to nanotubes, liquid crystals, and biosupramolecular electronics. *Acc. Chem. Res. 46*, 2498−2512.

(9) Mimuro, M., Nozawa, T., Tamai, N., Shimada, K., Yamazaki, I., Lin, S., Knox, R. S., Wittmershaus, B. P., Brune, D. C., and Blankenship, R. E. (1989) Excitation energy flow in chlorosome antennas of green photosynthetic bacteria. *J. Phys. Chem. 93*, 7503−7509.

(10) Didraga, C., and Knoester, J. (2003) Absorption and dichroism spectra of cylindrical J aggregates and chlorosomes of green bacteria. *J. Lumin. 102−103*, 60−66.

(11) Holzwarth, A. R., and Schaffner, K. (1994) On the structure of bacteriochlorophyll molecular aggregates in the chlorosomes of green bacteria. A molecular modelling study. *Photosynth. Res. 41*, 225−233.

(12) Kim, H., Li, H., Maresca, J. A., Bryant, D. A., and Savikhin, S. (2007) Triplet exciton formation as a novel photoprotection mechanism in chlorosomes of *Chlorobium tepidum*. *Biophys. J. 93*, 192−201.

(13) Tang, K. H., Zhu, L., Urban, V. S., Collins, A. M., Biswas, P., and Blankenship, R. E. (2011) Temperature and ionic strength effects on the chlorosome light-harvesting antenna complex. *Langmuir 27*, 4816−4828.

(14) Tang, J. K., Xu, Y., Muhlmann, G. M., Zare, F., Khin, Y., and Tam, S. W. (2013) Temperature shift effect on the *Chlorobaculum tepidum* chlorosomes. *Photosynth. Res. 115*, 23−41.

(15) Nozawa, T., Suzuki, M., Ohtomo, K., Morishita, Y., Konami, H., and Madigan, M. T. (1991) Aggregation structure of bacteriochlorophyll *c* in chlorosomes from *Chlorobium tepidum*. *Chem. Lett.*, 1641−1644.
(16) Nozawa, T., Ohtomo, K., Suzuki, M., Nakagawa, H., Shikama, Y., Konami, H., and Wang, Z. Y. (1994) Structures of chlorosomes and aggregated BChl *c* in *Chlorobium tepidum* from solid state high resolution CP/MAS ^{13}C NMR. *Photosynth. Res. 41*, 211−223.
(17) Balaban, T. S., Holzwarth, A. R., Schaffner, K., Boender, G. J., and de Groot, H. J. (1995) CP-MAS ^{13}C-NMR dipolar correlation spectroscopy of ^{13}C-enriched chlorosomes and isolated bacteriochlorophyll *c* aggregates of *Chlorobium tepidum*: The self-organization of pigments is the main structural feature of chlorosomes. *Biochemistry 34*, 15259−15266.
(18) Wang, Z. Y., Umetsu, M., Kobayashi, M., and Nozawa, T. (1999) Complete assignment of ^{1}H NMR spectra and structural analysis of intact bacteriochlorophyll *c* dimer in solution. *J. Phys. Chem. B 103*, 3742−3753.
(19) van Rossum, B. J., Steensgaard, D. B., Mulder, F. M., Boender, G. J., Schaffner, K., Holzwarth, A. R., and deGroot, H. J. (2001) A refined model of the chlorosomal antennae of the green bacterium *Chlorobium tepidum* from proton chemical shift constraints obtained with high-field 2-D and 3-D MAS NMR dipolar correlation spectroscopy. *Biochemistry 40*, 1587−1595.
(20) Egawa, A., Fujiwara, T., Mizoguchi, T., Kakitani, Y., Koyama, Y., and Akutsu, H. (2007) Structure of the light-harvesting bacteriochlorophyll *c* assembly in chlorosomes from *Chlorobium limicola* determined by solid-state NMR. *Proc. Natl. Acad. Sci. U.S.A. 104*, 790−795.
(21) Ganapathy, S., Oostergetel, G. T., Wawrzyniak, P. K., Reus, M., Gomez Maqueo Chew, A., Buda, F., Boekema, E. J., Bryant, D. A., Holzwarth, A. R., and de Groot, H. J. (2009) Alternating *syn-anti* bacteriochlorophylls form concentric helical nanotubes in chlorosomes. *Proc. Natl. Acad. Sci. U.S.A. 106*, 8525−8530.
(22) Kakitani, Y., Koyama, Y., Shimoikeda, Y., Nakai, T., Utsumi, H., Shimizu, T., and Nagae, H. (2009) Stacking of bacteriochlorophyll *c* macrocycles in chlorosome from *Chlorobium limicola* as revealed by intermolecular ^{13}C magnetic-dipole correlation, X-ray diffraction, and quadrupole coupling in ^{25}Mg NMR. *Biochemistry 48*, 74−86.
(23) Ganapathy, S., Oostergetel, G. T., Reus, M., Tsukatani, Y., Gomez Maqueo Chew, A., Buda, F., Bryant, D. A., Holzwarth, A. R., and de Groot, H. J. (2012) Structural variability in wild-type and *bchQ bchR* mutant chlorosomes of the green sulfur bacterium *Chlorobaculum tepidum*. *Biochemistry 51*, 4488−4498.
(24) Gomez Maqueo Chew, A., Frigaard, N. U., and Bryant, D. A. (2007) Bacteriochlorophyllide *c* C-8^{2} and C-12^{1} methyltransferases are essential for adaptation to low light in *Chlorobaculum tepidum*. *J. Bacteriol. 189*, 6176−6184.
(25) Lakshminarayana, R., Raju, M., Krishnakantha, T. P., and Baskaran, V. (2005) Determination of major carotenoids in a few Indian leafy vegetables by high-performance liquid chromatography. *J. Agric. Food Chem. 53*, 2838−2842.
(26) Metz, G., Wu, X. L., and Smith, S. O. (1994) Ramped-amplitude cross polarization in magic-angle-spinning NMR. *J. Magn. Reson., Ser. A 110*, 219−227.
(27) Bennett, A. E., Rienstra, C. M., Griffiths, J. M., Zhen, W., Lansbury, P. T., and Griffin, R. G. (1998) Homonuclear radio frequency-driven recoupling in rotating solids. *J. Chem. Phys. 108*, 9463−9479.
(28) Terry, G., David, B. B., and Mark, S. C. (1990) New, compensated Carr-Purcell sequences. *J. Magn. Reson. 89*, 479−484.
(29) Bennett, A. E., Rienstra, C. M., Auger, M., Lakshmi, K. V., and Griffin, R. G. (1995) Heteronuclear Decoupling in Rotating Solids. *J. Chem. Phys. 103*, 6951−6958.
(30) Adolphs, J., and Renger, T. (2006) How proteins trigger excitation energy transfer in the FMO complex of green sulfur bacteria. *Biophys. J. 91*, 2778−2797.
(31) Bartczak, A., Dudkowiak, A., and Frackowiak, D. (2003) Dipole strengths of the Qy(0,0) bacteriochlorophyll *c* transition. *Photochem. Photobiol. 78*, 525−528.
(32) Mitsuo, U., Hollander, J. G., Matysik, J., Wang, Z. Y., Adschiri, T., Nozawa, T., and de Groot, H. J. (2004) Magic-angle spinning nuclear magnetic resonance under ultrahigh field reveals two forms of intermolecular interaction within CH_2Cl_2-treated (3^1R)-type bacteriochlorophyll *c* solid aggregate. *J. Phys. Chem. B 108*, 2726−2734.
(33) Morgan-Kiss, R. M., Chan, L. K., Modla, S., Weber, T. S., Warner, M., Czymmek, K. J., and Hanson, T. E. (2009) *Chlorobaculum tepidum* regulates chlorosome structure and function in response to temperature and electron donor availability. *Photosynth. Res. 99*, 11−21.
(34) Takaichi, S., and Oh-oka, H. (1999) Pigment composition in the reaction center complex from the thermophilic green sulfur bacterium, *Chlorobium tepidum*: Carotenoid glucoside esters, menaquinone and chlorophylls. *Plant Cell Physiol. 40*, 691−694.
(35) Schmidt, K. (1980) Comparative study on the composition of chlorosomes (*Chlorobium* vesicles) and cytoplasmic membranes from *Chloroflexus aurantiacus* strain Ok-70-fl and *Chlorobium limicola f. thiosulfatophilum* strain 6230. *Arch. Microbiol. 124*, 21−31.
(36) Takaichi, S., Wang, Z. Y., Umetsu, M., Nozawa, T., Shimada, K., and Madigan, M. T. (1997) New carotenoids from the thermophilic green sulfur bacterium *Chlorobium tepidum*: 1′,2′-Dihydro-γ-carotene, 1′,2′-dihydrochlorobactene, and OH-chlorobactene glucoside ester, and the carotenoid composition of different strains. *Arch. Microbiol. 168*, 270−276.
(37) Dorssen, R. J., Vasmel, H., and Amesz, J. (1986) Pigment organization and energy transfer in the green photosynthetic bacterium *Chloroflexus aurantiacus*. II. The chlorosome. *Photosynth. Res. 9*, 33−45.
(38) Arellano, J. B., Psencik, J., Borrego, C. M., Ma, Y. Z., Guyoneaud, R., Garcia-Gil, J., and Gillbro, T. (2000) Effect of carotenoid biosynthesis inhibition on the chlorosome organization in *Chlorobium phaeobacteroides* strain CL1401. *Photochem. Photobiol. 71*, 715−723.
(39) Moss, G. P. (1976) Carbon-13 NMR spectra of carotenoids. *Pure Appl. Chem. 47*, 97−102.
(40) Ildefonse, P., Calas, G., Flank, A. M., and Lagarde, P. (1995) Low Z elements (Mg, Al, and Si) K-edge X-ray absorption spectroscopy in minerals and disordered systems. *Nucl. Instrum. Methods Phys. Res., Sect. B 97*, 172−175.
(41) Li, D., Peng, M., and Murata, T. (1999) Coordination and local structure of magnesium in silicate minerlas and glasses: Mg *K*-edge XANES study. *Can. Mineral. 37*, 199−206.
(42) Trcera, N., Cabaret, D., Rossano, S., Farges, F., Flank, A. M., and Lagarde, P. (2009) Experimental and theoretical study of the structural environment of magnesium in minerals and silicate glasses using X-ray absorption near-edge structure. *Phys. Chem. Miner. 36*, 241−257.
(43) Kluge, S., and Weston, J. (2005) Can a hydroxide ligand trigger a change in the coordination number of magnesium ions in biological systems? *Biochemistry 44*, 4877−4885.
(44) Balaban, T. S. (2005) High-five for Mg complex. *Chem. Eng. News 83*, 6.
(45) Cabaret, D., Sainctavit, P., Ildefonse, P., and Flank, A. M. (1998) Full multiple scattering calculations of the X-ray absorption near edge structure at the magnesium K-edge in pyroxene. *Am. Mineral. 83*, 300−304.
(46) Maresca, J. A., Gomez Maqueo Chew, A., Ponsati, M. R., Frigaard, N. U., Ormerod, J. G., and Bryant, D. A. (2004) The *bchU* gene of *Chlorobium tepidum* encodes the C-20 methyltransferase in bacteriochlorophyll *c* biosynthesis. *J. Bacteriol. 186*, 2558−2566.
(47) Harada, J., Mizoguchi, T., Tsukatani, Y., Noguchi, M., and Tamiaki, H. (2012) A seventh bacterial chlorophyll driving a large light-harvesting antenna. *Sci. Rep. 2*, 671.
(48) Vogl, K., Tank, M., Orf, G. S., Blankenship, R. E., and Bryant, D. A. (2012) Bacteriochlorophyll *f*: Properties of chlorosomes containing the "forbidden chlorophyll". *Front. Microbiol. 3*, 298.

(49) *The PyMOL Molecular Graphics System*, version 1.5.0.4. Schrödinger, LLC, Portland, OR.
(50) Brune, D. C., Nozawa, T., and Blankenship, R. E. (1987) Antenna organization in green photosynthetic bacteria. 1. Oligomeric bacteriochlorophyll *c* as a model for the 740 nm absorbing bacteriochlorophyll *c* in *Chloroflexus aurantiacus* chlorosomes. *Biochemistry 26*, 8644−8652.
(51) Nozawa, T., Noguchi, T., and Tasumi, M. (1990) Resonance Raman studies on the structure of bacteriochlorophyll *c* in chlorosomes from *Chloroflexus aurantiacus*. *J. Biochem. 108*, 737−740.
(52) Hildebrandt, P., Tamiaki, H., Holzwarth, A. R., and Schaffner, K. (1994) Resonance Raman spectroscopic study of metallochlorin aggregates. Implications for the supramolecular structure of chlorosomal bacteriochlorophyll *c* antennae of green bacteria. *J. Phys. Chem. 98*, 2191−2197.
(53) Chiefari, J., Griebenow, K., Griebenow, N., Balaban, T. S., Holzwarth, A. R., and Schaffner, K. (1995) Models for the pigment organization in the chlorosomes of photosynthetic bacteria: Diastereoselective control of *in vitro* bacteriochlorophyll c_S aggregation. *J. Phys. Chem. 99*, 1357−1365.
(54) Sato, H., Uehara, K., Ishii, T., and Ozaki, Y. (1995) Near-infrared-FT-Raman study of aggregation of bacteriochlorophyll *c* in whole living *Chlorobium limicola*. *Photochem. Photobiol. 62*, 509−513.
(55) Jochum, T., Reddy, C. M., Eichhofer, A., Buth, G., Szmytkowski, J., Kalt, H., Moss, D., and Balaban, T. S. (2008) The supramolecular organization of self-assembling chlorosomal bacteriochlorophyll *c*, *d*, or *e* mimics. *Proc. Natl. Acad. Sci. U.S.A. 105*, 12736−12741.
(56) Kasha, M., Rawls, H. R., and El-Bayoumi, A. M. (1965) The exciton model in molecular spectroscopy. *Pure Appl. Chem. 11*, 371−392.
(57) Kobayashi, T. (1996) *J-aggregates*, World Scientific, Singapore.
(58) van Amerongen, H., Valkunas, L., and van Grondelle, R. (2000) *Photosynthetic excitons*, World Scientific, Singapore.
(59) Didraga, C., and Knoester, J. (2004) Optical spectra and localization of excitons in inhomogeneous helical cylindrical aggregates. *J. Chem. Phys. 121*, 10687−10698.
(60) Wang, Z. Y., Umetsu, M., Kobayashi, M., and Nozawa, T. (1999) ^{13}C- and ^{15}N-NMR studies on the intact bacteriochlorophyll *c* dimers in solutions. *J. Am. Chem. Soc. 121*, 9363−9369.
(61) Mizoguchi, T., Hara, K., Nagae, H., and Koyama, Y. (2000) Structural transformation among the aggregate forms of bacteriochlorophyll *c* as determined by electronic-absorption and NMR spectroscopies: Dependence on the stereoisomeric configuration and on the bulkiness of the 8-C side chain. *Photochem. Photobiol. 71*, 596−609.
(62) Wang, Y., Freund, D. M., Magdaong, N. M., Urban, V. S., Frank, H. A., Hegeman, A. D., and Tang, J. K. (2014) Impact of esterified bacteriochlorophylls on the biogenesis of chlorosomes in *Chloroflexus aurantiacus*. *Photosynth. Res.*, DOI: 10.1007/s11120-014-0017-5.
(63) Staehelin, L. A., Golecki, J. R., and Drews, G. (1980) Supramolecular organization of chlorosomes (*Chlorobium* vesicles) and of their membrane attachment sites in *Chlorobium limicola*. *Biochim. Biophys. Acta 589*, 30−45.
(64) Hohmann-Marriott, M. F., Blankenship, R. E., and Roberson, R. W. (2005) The ultrastructure of *Chlorobium tepidum* chlorosomes revealed by electron microscopy. *Photosynth. Res. 86*, 145−154.
(65) Psencik, J., Ikonen, T. P., Laurinmaki, P., Merckel, M. C., Butcher, S. J., Serimaa, R. E., and Tuma, R. (2004) Lamellar organization of pigments in chlorosomes, the light harvesting complexes of green photosynthetic bacteria. *Biophys. J. 87*, 1165−1172.